J Electr Eng Technol.2017; 13(?): 1921-718
http://doi.org/10.???/JEET.2017.13.1.1921

ISSN(Print) 1975-0102
ISSN(Online) 2093-7423

Smart Air Condition Load Forecasting based on Thermal Dynamic Model and Finite Memory Estimation for Peak-energy Distribution

Hyun Duck Choi*, Soon Woo Lee†, Dong Sung Pae*, Sung Hyun You* and Myo Taeg Lim*

Abstract – In this paper, we propose a new load forecasting method for smart air conditioning (A/C) based on the modified thermodynamics of indoor temperature and the unbiased finite memory estimator (UFME). Based on modified first-order thermodynamics, the dynamic behavior of indoor temperature can be described by the time-domain state-space model, and an accurate estimate of indoor temperature can be achieved by the proposed UFME. In addition, a reliable A/C load forecast can be obtained using the proposed method. Our study involves the experimental validation of the proposed A/C load forecasting method and communication construction between DR server and HEMS in a test bed. Through experimental data sets, the effectiveness of the proposed estimation method is validated.

Keywords: Home energy management system(HEMS), Air condition(A/C), Demand response(DR), Unbiased finite memory estimation (UFME), Thermodynamic model

1. Introduction

With the advent of the smart grid project that offers a two-way communication infrastructure, a time-varying price can be provided to residential consumers individually. In reality, residential consumers have the potential to save money with time-varying electricity prices through the flexible operation of residential appliances [1-3]. Through a home energy management system (HEMS), residential consumers can manage their energy consumption of many residential appliances in response to dynamic pricing and participate in economic demand response (DR) [4-6]. A HEMS carries out optimal and automated load control for different types of load based on observation for the consumer's comfort, home environment, and electricity bills. The ability to provide intelligent solutions for energy consumption is the most important issue in the design of a HEMS.

One of the most complex tasks facing the smart grid project appears in energy demand forecasting. In particular, residential load forecasting is more difficult, because daily household consumption depends on the random nature of turning appliances on/off and consumers' specific lifestyles [7-9].

However, accurate forecasting for appliance load is necessary when balancing between electricity supply and demand. With the increased proportion of houses with smart meters installed in many countries and DR support [10, 11], there have been several efforts to perform accurate load forecasting for residential appliances to ensure the efficient consumption of electrical energy. In particular, modeling home appliance loads plays an important role, since it is the first step to understanding and forecasting residential electricity consumption data. Many studies on load forecasting for residential appliances have been conducted over the years, and it remains a key factor of smart grid technology.

Peak demand periods and worst cases such as blackouts usually occur during the summer or winter, because of the excessive use of thermal appliances (e.g., air conditioning [A/C] or electric heaters) by residential consumers. Many studies have shown that thermostatically controlled appliances have a significant effect on peak demand; thus, changes in the consumption pattern of thermal appliances is effective at saving costs in electricity bills and reducing overall peak demand, which is essential for utility and grid providers. The most common thermostatically controlled household appliance is the residential A/C, which occupies a significant portion of residential load consumption [12-14]. There are several studies about scheduling A/C by anticipating the thermodynamics [15-17] of the indoor temperature. These results emphasize that the model- based analysis of indoor temperature gives efficient load control for thermodynamics appliances, because estimating the indoor temperature is essential for load forecasting of thermodynamics appliances in a household. In addition, an efficient DR reaction can be achieved by offering consumers temperature information before and after DR reactions.

In recent years, considerable attention and effort have been given to the design of finite memory state estimation (FMSE) as an alternative to infinite impulse response (IIR)-type estimation [18-22]. Because IIR-type estimation uses all past input/output information to produce state

† Corresponding Author: Korea Electrotechnology Research Institute (KERI), Korea. (rheesw@keri.re.kr)
* School of Electrical Engineering, Korea University, Korea. (chlgusejr87, paeds915, ysh88, mlim@korea.ac.kr)
Received: December 2, 2016; Accepted: September 26, 2017

estimates, poor estimation performance or divergence may be exhibited due to the accumulation of modeling and computational errors [23, 24]. While the Kalman filter may exhibit poor performance or even divergence if the system has more model parameter uncertainty, FIR filters have robustness against model parameter uncertainty and incorrect noise information. Furthermore, FMSE can prevent error accumulation problem because it only uses recent finite measurements and shows superior reliability. In addition, given its structural characteristics, the advantages of FMSE include bounded-input bounded-output (BIBO) stability and robustness against temporary model uncertainties, incorrect noise information, and quantization effects. FMSE may be used independently or combined with IIR estimator to overcome its disadvantages [31, 32]. Despite these advantages, the existing literature does not yet include studies that have focused on the estimation of indoor temperature using FMSE; this lack of effective research results motivates this study.

Since residential A/C consumption significantly affects peak demand, the development of residential A/C load forecasting is imperative. In this paper, we provide a new A/C load consumption forecasting approach based on the accurate estimation of indoor temperature to accomplish accurate and reliable A/C load forecasting and avoid the lack of emergency power reserves during peak hours. While there are extensive results for large facilities, there are limited results in open literature for suburban residential homes. Thus, we implement HEMS in our laboratory and provide verification of both the proposed A/C load forecasting method and communication architecture environment.

2. Estimation of Indoor Temperature

2.1 Modified thermodynamics of indoor temperature

As a standard analysis of thermodynamics including a residential A/C, the discrete time thermodynamics of indoor temperature [7] can be described as follows

$$\begin{aligned} T_{in}(k+1) &= T_{in}(k) + \alpha\left(T_{out}(k) - T_{in}(k)\right) \\ &+ \beta P_{AC}(k) + c + w(k), \end{aligned} \tag{1}$$

where $T_{in}(k)$, $T_{out}(k)$, and $P_{AC}(k)$ denote the indoor temperature, outdoor temperature, and electricity power consumed by the A/C, respectively, and $w(k)$ denotes white Gaussian noise. α, β and c are thermal parameters to be estimated. The validity of the standard model was verified based on the experimental data sets collected in our laboratory, which include the indoor temperature, outdoor temperature, and A/C power usage patterns. However, the standard thermodynamics could not properly model the indoor temperature of our laboratory because the impact of the internal thermal noise is simply described by the constant scalar c. It is necessary for the model to offer a more detailed description of the impact of internal thermal noise; thus, we introduce modified thermodynamics as follows:

$$\begin{aligned} T_{in}(k+1) &= T_{in}(k) + \alpha\left(T_{out}(k) - T_{in}(k)\right) \\ &+ \beta P_{AC}(k) + \chi\left(\gamma - T_{in}(k)\right) + w(k), \end{aligned} \tag{2}$$

where γ and χ are the additional thermal parameters for modified thermodynamic model. The main difference between the traditional and proposed model is the terms of the internal thermal noise. The impact of internal thermal noise is expressed by the term $(\gamma - T_{in}(k))$. The next point in the indoor temperature $T_{in}(k+1)$ is influenced by the difference between internal thermal noise γ and $T_{in}(k)$. γ represents the temperature of the internal thermal noise; using the modified dynamic in (2), the state-space model can be easily derived as

$$\begin{aligned} x_{k+1} &= Ax_k + Bu_k + w_k, \\ y_k &= Cx_k + v_k, \end{aligned} \tag{3}$$

where $x_k = y_k = T_{in}(k)$, $u_k = \left[T_{out}(k)\ P_{AC}(k)\ 1\right]^T$, $v(k)$ denotes the thermometer noise that is white Gaussian, and the state-space matrices are represented as

$$A = 1 - \alpha - \chi,\ B = \left[\alpha\ \ \beta\ \ \chi\gamma\right],\ C = 1. \tag{4}$$

Using the least-square (LS) algorithm, the estimation of model parameter (4) can be obtained.

$$\left(\hat{A}, \hat{B}\right) = \arg\min_{A,B}\left\{\sum_{k=1}^{\mathbb{N}}\left\|x_{k+1} - \left(Ax_k + Bu_k\right)\right\|^2\right\}, \tag{5}$$

where $\hat{A}$ and $\hat{B}$ are estimates of the parameter matrices and $\mathbb{N}$ is the number of measurements for parameter identification. We can validate the accuracy of the model using different experimental data sets based on the extracted parameter matrices. The indoor temperature can be estimated by the state-space model with the extracted parameters.

$$\hat{x}_{k+1} = \hat{A}\hat{x}_k + \hat{B}u_k + w_k. \tag{6}$$

where $\hat{x}_k$ is the modified model-based estimate of the indoor temperature. The model accuracy can be measured by the mean squared prediction error (PE) e_p, which is given by

$$e_p = \frac{1}{\mathbb{N}}\sum_{k=1}^{\mathbb{N}}\left\|\hat{x}_{k+1} - x_{k+1}\right\|^2. \tag{7}$$

The indoor temperature estimation-based modified

thermodynamic model is evaluated in Section 3.

2.2 Finite memory estimation of the indoor temperature

Although the state-space model of modified thermodynamics (3) can offer a more detailed description of indoor temperature, a modeling error still exists and may cause poor estimation performance. In our previous work [31], we proposed a new digital phase-locked loop with finite-memory structure called the unbiased finite-memory DPLL (UFMDPLL) and showed excellent robustness performance against incorrect noise information. Among the same line of the idea in [31], we extended the approach to the control problem of the indoor temperature and proposed a new load forecasting method for smart air conditioning by using the unbiased finite-memory estimator.

Thus, we propose an unbiased finite memory estimator (UFME) with considering control input ... in this section to mitigate the accumulation of modeling and computational errors. We define the horizon size of the UFME as N. On the most recent time horizon $[k-N, k-1]$, the finite number of control inputs and measurements on the horizon $[k-N;k-1]$ for UFME are constructed as

$$Y_{k-1} \triangleq \left[y_{k-N}^T \, y_{k-N+1}^T \cdots y_{k-1}^T \right]^T,$$
$$U_{k-1} \triangleq \left[u_{k-N}^T \, u_{k-N+1}^T \cdots u_{k-1}^T \right]^T.$$

The UFME is proposed based on the state space model (6) in the following theorem:

Theorem 1. Given $N \geqslant 2$, the UFME of the indoor temperature $\hat{x}_k^f$ is given by

$$\hat{x}_k^f = \mathcal{H} Y_{k-1} + \mathcal{L} U_{k-1}, \tag{8}$$

where

$$\mathcal{H} \triangleq \left[h_1 \, h_2 \cdots h_N \right], \; h_i = \left(\frac{1-\hat{A}^2}{\hat{A}^{-2N}-1} \right) \hat{A}^{i-1-N}$$
$$\mathcal{L} \triangleq -\mathcal{H} \begin{bmatrix} \hat{A}^{-1}\hat{B} & \hat{A}^{-2}\hat{B} & \cdots & \hat{A}^{-N}\hat{B} \\ 0 & \hat{A}^{-1}\hat{B} & \cdots & \hat{A}^{-N+1}\hat{B} \\ \vdots & \vdots & \vdots & \vdots \\ 0 & 0 & \cdots & \hat{A}^{-1}\hat{B} \end{bmatrix}, \tag{9}$$
$$i = 1, 2, \cdots, N.$$

Proof. The state space model (3) can be rewritten in a batch form on the horizon $[k-N, k]$ as follows:

$$x_k = \hat{A}^N x_{k-N} + \hat{B}_N U_{k-1} + \hat{M}_N W_{k-1}, \tag{10}$$

$$Y_{k-1} = \tilde{C}_N x_{k-N} + \tilde{B}_N U_{k-1} + \tilde{G}_N W_{k-1} + V_{k-1}, \tag{11}$$

where

$$W_{k-1} \triangleq \left[w_{k-N}^T \, w_{k-N+1}^T \cdots w_{k-1}^T \right]^T,$$
$$V_{k-1} \triangleq \left[v_{k-N}^T \, v_{k-N+1}^T \cdots v_{k-1}^T \right]^T,$$
$$\hat{B}_N = \left[\hat{A}^{N-1}\hat{B} \;\; \hat{A}^{N-2}\hat{B} \cdots \hat{B} \right],$$
$$\hat{M}_N = \left[\hat{A}^{N-1} \;\; \hat{A}^{N-2} \cdots 1 \right],$$
$$\tilde{C}_N \triangleq \left[1 \quad \hat{A} \quad \hat{A}^2 \quad \cdots \quad \hat{A}^{N-1} \right]^T,$$
$$\tilde{B}_N \triangleq \begin{bmatrix} 0 & 0 & \cdots & 0 & 0 \\ \hat{B} & 0 & \cdots & 0 & 0 \\ \hat{A}\hat{B} & \hat{B} & \cdots & 0 & 0 \\ \vdots & \vdots & \vdots & \vdots & \vdots \\ \hat{A}^{N-2}\hat{B} & \hat{A}^{N-3}\hat{B} & \cdots & \hat{B} & 0 \end{bmatrix},$$
$$\tilde{G}_N \triangleq \begin{bmatrix} 0 & 0 & \cdots & 0 & 0 \\ 1 & 0 & \cdots & 0 & 0 \\ \hat{A} & 1 & \cdots & 0 & 0 \\ \vdots & \vdots & \vdots & \vdots & \vdots \\ \hat{A}^{N-2} & \hat{A}^{N-3} & \cdots & 1 & 0 \end{bmatrix}, \tag{12}$$

(10) can be rewritten as

$$x_{k-N} = \hat{A}^{-N} x_k - \hat{A}^{-N} \hat{B}_N U_{k-1} - \hat{A}^{-N} \hat{M}_N W_{k-1}. \tag{13}$$

By substituting (13) into (11), we obtain

$$\begin{aligned} Y_{k-1} &= \tilde{C}_N (\hat{A}^{-N} x_k - \hat{A}^{-N} \hat{B}_N U_{k-1} - \hat{A}^{-N} \hat{M}_N W_{k-1}) \\ &\quad + \tilde{B}_N U_{k-1} + \tilde{G}_N W_{k-1} + V_{k-1} \\ &= \tilde{C}_N \hat{A}^{-N} x_k + (\tilde{B}_N - \tilde{C}_N \hat{A}^{-N} \hat{B}_N) U_{k-1} \\ &\quad + (\tilde{G}_N - \tilde{C}_N \hat{A}^{-N} \hat{M}_N) W_{k-1} + V_{k-1} \\ &= \bar{C}_N x_k + \bar{B}_N U_{k-1} + \bar{G}_N W_{k-1} + V_{k-1}, \end{aligned} \tag{14}$$

where

$$\bar{C}_N \triangleq \tilde{C}_N \hat{A}^{-N} = \left[\hat{A}^{-N} \quad \hat{A}^{1-N} \quad \hat{A}^{2-N} \quad \cdots \quad \hat{A}^{-1} \right]^T,$$
$$\bar{B}_N \triangleq \tilde{B}_N - \tilde{C}_N \hat{A}^{-N} \hat{B}_N = \begin{bmatrix} \hat{A}^{-1}\hat{B} & \hat{A}^{-2}\hat{B} & \cdots & \hat{A}^{-N}\hat{B} \\ 0 & \hat{A}^{-1}\hat{B} & \cdots & \hat{A}^{-N+1}\hat{B} \\ \vdots & \vdots & \vdots & \vdots \\ 0 & 0 & \cdots & \hat{A}^{-1}\hat{B} \end{bmatrix}, \tag{15}$$
$$\bar{G}_N \triangleq \tilde{G}_N - \tilde{C}_N \hat{A}^{-N} \hat{M}_N = \begin{bmatrix} \hat{A}^{-1} & \hat{A}^{-2} & \cdots & \hat{A}^{-N} \\ 0 & \hat{A}^{-1} & \cdots & \hat{A}^{-N+1} \\ \vdots & \vdots & \vdots & \vdots \\ 0 & 0 & \cdots & \hat{A}^{-1} \end{bmatrix}.$$

(8) can be written as

$$\begin{aligned}\hat{x}_k^f &= \mathcal{H}Y_{k-1} + \mathcal{L}U_{k-1},\\ &= \mathcal{H}(\bar{C}_N x_k + \bar{B}_N U_{k-1} + \bar{G}_N W_{k-1} + V_{k-1}) + \mathcal{L}U_{k-1}\\ &= \mathcal{H}\bar{C}_N x_k + \mathcal{H}\bar{B}_N U_{k-1} + \mathcal{L}U_{k-1} + \mathcal{H}\bar{G}_N W_{k-1} + \mathcal{H}V_{k-1}.\end{aligned} \quad (16)$$

The expectation is taken on both sides of (16) as follows: $E[\hat{x}_k^f] = \mathcal{H}\bar{C}_N E[x_k] + (\mathcal{H}\bar{B}_N + \mathcal{L})U_{k-1}$. The unbiasedness (or deadbeat) condition $E[\hat{x}_k^f] = E[x_k]$ can be ensured by taking

$$\mathcal{H}\bar{C}_N = 1, \quad \mathcal{H}\bar{B}_N = -\mathcal{L}. \quad (17)$$

Many solutions can generally be obtained to (17) by analyzing $\bar{C}_N$ and $\mathcal{H}$. We consider a solution $\mathcal{H}$ that minimizes $\sum_{i=1}^{N} h_i^2$ subject to (17) in the Moore-Penrose sense. (17) can be represented by

$$\mathcal{H}\bar{C}_N = \begin{bmatrix} h_1 & h_2 & \cdots & h_N \end{bmatrix} \begin{bmatrix} \hat{A}^{-N} \\ \hat{A}^{1-N} \\ \hat{A}^{2-N} \\ \vdots \\ \hat{A}^{-1} \end{bmatrix} = \sum_{i=1}^{N} h_i \hat{A}^{i-1-N} = 1 \quad (18)$$

Introduce the following Lagrange function:

$$f = \sum_{i=1}^{N} h_i^2 + \lambda \left\{ 1 - \sum_{i=1}^{N} h_i \hat{A}^{i-1-N} \right\}, \quad (19)$$

where λ represents the Lagrange multipliers. The derivative of (19) with respect to h_i gives

$$\frac{\partial f}{\partial h_i} = \sum_{i=1}^{N} \left\{ 2h_i - \lambda \hat{A}^{i-1-N} \right\} = 0, \quad (20)$$

which leads to

$$h_i = \frac{\lambda \hat{A}^{i-1-N}}{2}. \quad (21)$$

By substituting (18) into (21), we obtain

$$\frac{\lambda}{2} \sum_{i=1}^{N} \hat{A}^{2i-2-2N} = \frac{\lambda}{2} \left(\frac{\hat{A}^{-2N} - 1}{1 - \hat{A}^2} \right) = 1. \quad (22)$$

From (22), we obtain λ as follows:

$$\lambda = 2 \left(\frac{1 - \hat{A}^2}{\hat{A}^{-2N} - 1} \right). \quad (23)$$

Finally, by substituting (23) into (21), h_i is obtained.

$$h_i = \left(\frac{1 - \hat{A}^2}{\hat{A}^{-2N} - 1} \right) \hat{A}^{i-1-N}, \quad i = 1, 2, \cdots, N. \quad (24)$$

This completes the proof.

Remark 1. It should be noted that $\mathcal{H}$ is independent of the noise information and initial state. In other words, given N, $\mathcal{H}$ is always a constant matrix even if the noise information is uncertain or incorrect.

Remark 2. The proposed UFME can prevent the accumulation of modeling and computational errors because it only uses recent finite measurement. The gain matrix of the UFME was obtained using the Moore-Penrose pseudo inverse and Lagrange equation, and it can minimize the bad effects caused by modeling and computational errors. Thus, the proposed UFME becomes an effective approach when there is incorrect noise information or numerical errors in a model.

3. Experimental Results

3.1 Scenarios

The whole scenario under consideration is shown in Fig. 1. The provider will determine the DR signal based on the estimation of A/C load consumption. The DR signal, which consists of the total energy reductions of each household, the estimated peak hours, and the electricity price, is calculated and transmitted to each household based on this information. The HEMS, in each household will provide the proper A/C load consumption by scheduling appliance operation times considering the electricity bill, the reduction in peak demand, and user comfort. This means that the HEMS in each individual residence will estimate the A/C load consumption based on the estimated indoor

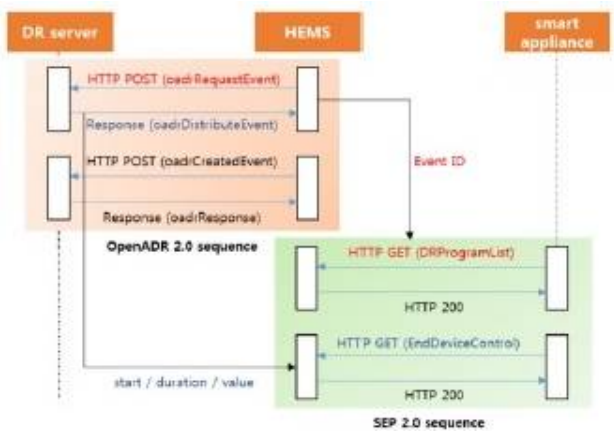

Fig. 1. Message conversion between SEP 2.0 and OpenADR 2.0a

temperature. Then, each HEMS decides whether to reduce the power according to user preference for a trade-off between the electricity bill and user comfort. It is assumed that the additional incentive for maintaining the pre-contract DR level is offered to customers to encourage the residential customers to participate the DR service. The standardization of communication and data format is required to stimulate this DR service.

Remark 3. OpenADR has been developed based on the Energy Interoperation (EI), which provides a protocol authentication program. OpenADR 2.0 protocol defines the profile of a common information exchange between demand response providers and their consumers, and it describes the basic operation of an upper-layer service [25-27]. It uses HyperText Transfer Protocol (HTTP).

Remark 4. SEP 2.0 mainly explains the various services related to demand response, which are defined in Demand Response and Load Control (DRLC) and the operation of the resource center for energy-related devices on the premises [28]-[30]. SEP 2.0 protocol located at a top-tier IP stack developed by the ZigBee with the HomePlug Alliance. It transmits data in eXtensible Mark-up Language (XML) format, that is type of demand response message, using HTTP based on REpresentation State Transfer (REST) architecture by default.

Remark 5. The demand response system consists of the demand response servers, smart appliances, and HEMS. Demand response server includes of response service providers (e.g. power suppliers and load management operaters). The OpenADR 2.0 protocol ensures an automated demand response service and it is able to accept the role of network operator. It is accomplished by applying a pre-determined strategy to the system between the service provider and the consumer. Meanwhile, OpenADR 2.0 may serve as an external demand response server. The SEP 2.0 protocol cannot receive demand response messages from the demand response server, which is located outside of the home, because it defines various operations intended for energy devices in the home. Thus, in this paper, we design an automatic demand response system that includes OpenADR 2.0 and SEP 2.0. Based on OpenADR 2.0, demand response signals are transmitted between the server and the HEMS. At home, demand response services are performed for smart appliances based on SEP 2.0 protocols. Fig. 1 shows the message conversion in demand response system.

3.2 Experiment setup and validation

3.2.1 Experiment setup

The experimental setup is presented in this section. Fig. 2 illustrates the layout of the HEMS installation of the proposed indoor temperature and A/C forecast algorithm. For the practical validation of the proposed approach, we implemented the HEMS with a smart A/C in our laboratory and collected experimental measurement sets. The test bed is located in the research laboratory at the Department of Electrical Engineering at Korea University, and this 35 m2-test bed is designed to represent the actual living space. Fig. 3 shows the test bed and its setup environment. The LabJack Digit-TL thermostat is located at the center of the test bed. Detailed specifications of the equipment used for the HEMS are listed in Table 1. The smart AC used in our experiment can communicate with MCU via SEP 2.0 protocols. The MCU included a SEP 2.0 communication unit, a control unit for a smart A/C, and an A/C power measuring unit. The laptop communicated with the DR server through the Open ADR 2.0 standard, and measurement data sets were collected every 10 minutes from June to August in 2014 and 2015 in Korea for the experiment. The data sets included A/C power consumption, humidity, indoor

Table 1. Device configuration

Laptop			
model	processor	memory	OS
Lenovo ThinkPad E540	2.2GHz Intel i7-4702M Q	4GB	Windows7 32bit
MCU			
model	function	communication	performance
ATmega2560	communication with Server and A/C, controller	interface: RS232C communication level: TTL	CPU: 8-bit AVR Flash: 256KB
Smart A/C			
model	function	voltage	current
Carrier CPM-A157T GB0	Air Conditioner Dehumidifier	220V	8.1A

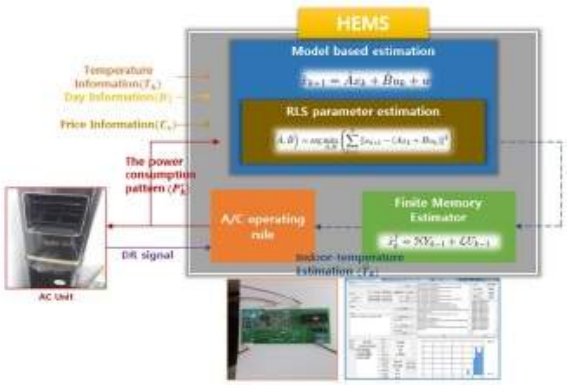

Fig. 2. Layout of HEMS

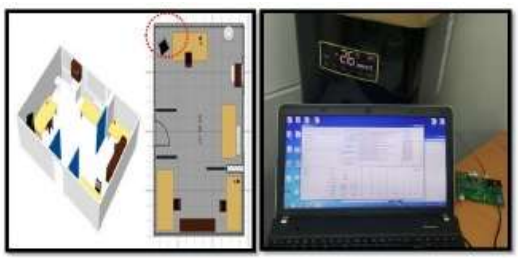

Fig. 3. Test bed and setup environment of HEMS

Table 2. Model parameters

$\hat{\alpha}$	$\hat{\beta}$	$\hat{\gamma}$	$\hat{\chi}$	$P_{AC}[k]$(kWh)
0.1176	2.0121	27.1269	0.5081	0.3

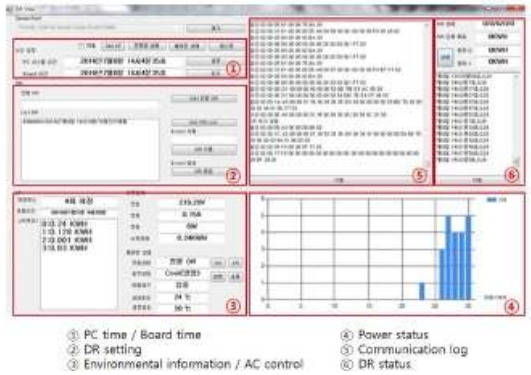

Fig. 4. Snapshot of the application program of HEMS

temperature, and outdoor temperature. Real indoor temperature and humidity information were collected using a LabJack Digit-TL thermostat, and we used the open source of the Korea Meteorological Administration to determine the day-ahead outdoor temperature. The snapshot of the application program of the HEMS is shown in Fig. 4 and the general pattern of the thermodynamic model has different characteristics for a typical day and a rainy day, which has an irregular pattern. Thus, we excluded rainy day data sets in this study to reduce the errors in the thermodynamic models. The number of observations N for model identification corresponds to 1, 3, and 7 days of measurement. Among them, 432 points (one point every 10 minutes) for three previous days were used for the identification of the thermal model parameters in this study. Based on this set, we obtained the modified thermodynamic model parameters by the least squares algorithm. Table 2 shows the model parameters. Using the collected parameter set and outdoor temperature, the proposed UFME based on Theorem 1 estimates the next-point indoor temperature. In this study, Q,R, and the horizon size N for UFME choose 0.7447; 0.3, and 10 points, respectively. The simulation and experiment data were mainly focused on a two-day period due to the limited space of the paper.

3.2.2 Experiment results

The experimental results are presented in this section and the performance of the proposed A/C load consumption forecasting approach is evaluated.

(a) Indoor temperature estimation

Fig. 5 shows the estimation of the indoor temperature based on the modified model and UFME. The proposed UFME, compared to the modified model-based estimation, could reduce estimation errors by 62.06%. Thus, the proposed UFME leads to a 62.06% improvement in estimation accuracy compared with the modified model-based estimation.

Table 3. A/C operating rule based on humidity and estimation of indoor temperature

minimum time of continuous operation	20 minutes
maximum time of continuous operation	4 hour
minimum operating time per day	8 hour
Temperature > 27 & humidity < 70%	Turn on
Temperature > 26 & humidity < 70%	Turn on

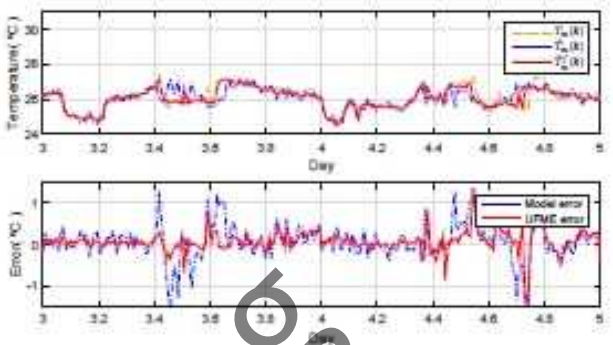

Fig. 5. Real measurement of indoor temperature and its estimation (top) and estimation error (bottom)

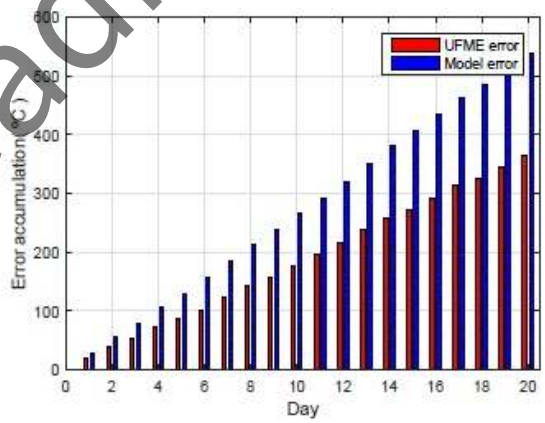

Fig. 6. Accumulated error over 20 days

(b) Error accumulation

The error accumulation during 20 days is shown in Fig. 6. These results show that the proposed UFME-based estimation is more robust against modeling error than the modified model-based estimation. After the accurate estimation of the indoor temperature, the next-point A/C load forecast can be obtained via the estimation information and the A/C operating rules. The A/C operating rules are listed in Table 3.

(c) A/C load forecasting

Figs. 7 and 8 show a comparison of A/C load forecasting between UFME and the model-based approach. As shown in the figures, the UFME-based approach provides

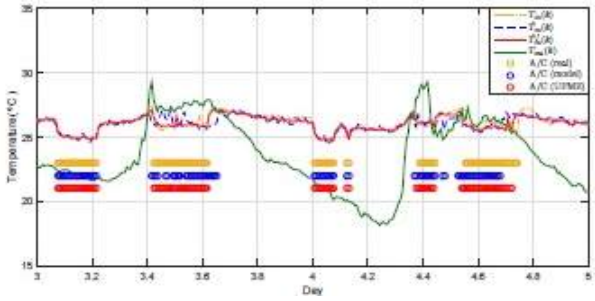

Fig. 7. Real A/C operation pattern and its estimation

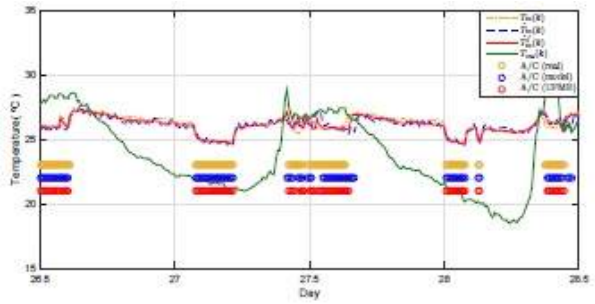

Fig. 8. Real A/C operation pattern and its estimation

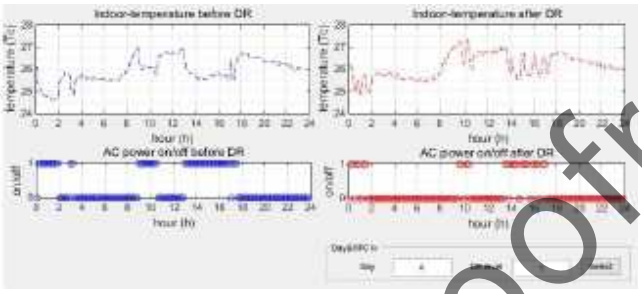

Fig. 9. Indoor temperature and A/C load consumption before and after DR

approximately 6.25% more accurate A/C on/off forecasting per day compared to the model-based approach. In particular, the prediction of A/C on/off based on UFME shows 16.67% more accuracy in the peak time (10:00-15:00). By providing an accurate prediction of A/C load consumption, the service provider carries out the operation of a correct and reliable smart grid system, and an efficient DR reaction can be achieved.

(d) Indoor Temperature and A/C operation

Fig. 9 shows the indoor temperature and A/C on/off action before and after receiving DR reduction information (DR level 1: 50% reduction). As shown in Fig. 7, a 50% intensive load reduction can be achieved during peak time. This study mainly focused on accurate A/C load estimation, which is meaningful information for load shifting or reducing techniques that seek to offer reliable service. AC usage after DR can be integrated into a convex optimization framework for optimal AC scheduling, which will be the subject of future work.

4. Conclusion

This paper proposed a new A/C load forecasting approach for the reliable estimation of residential A/C load consumption, and it is helpful for energy distribution at peak times. Based on the modified thermodynamics of indoor temperatures, a new UFME that uses recent finite measurements of the receding horizon and the correction term with the unbiasedness property is provided to estimate indoor temperatures. User patterns, the modified thermodynamics of indoor temperature, and the UFME were integrated in the HEMS to overcome the difficulties of the load forecasting of A/C due to its random nature of turning on/off. The proposed A/C load forecasting approach provides the accurate estimation of A/C load consumption. We implemented the HEMS, which includes the communication construction between the DR server and HEMS for demonstration purposes in a laboratory environment to verify the case study of estimating the smart A/C load consumption. The effectiveness of the proposed estimation method was validated based on real experimental data sets. The proposed A/C load estimation approach can be incorporated into the optimization problem for optimal A/C scheduling, and the ideas provided in this study can be broadened to control other thermal appliances, which will be the subject of our future work.

Acknowledgements

This work was supported by R&D Program of MOTIE/KEIT, Korea. The authors would like to thank the Ministry of Trade, Industry and Energy, Korea. (No: 10041779, Development of Energy Demand Response System for Smart Home).

References

[1] D.-M. Han and J.-H. Lim. Design and Implementation of Smart Home Energy Management Systems based on Zigbee. *IEEE Trans. Consumer Elect.,* vol. 56, no. 3, pp.1417–1425, 2010.

[2] G. T. Costanzo, G. Zhu, M. F. Anjos, and G. Savard. A System Architecture for Autonomous Demand Side Load Management in Smart Buildings. *IEEE Trans. Smart Grid*, vol. 3, no. 4, 2012.

[3] A. Mohsenian-Rad and A. Leon-Garcia. Optimal Residential Load Control with Price Prediction in Real-Time Electricity Pricing Environments. *IEEE Trans. Smart Grid*, vol. 1, no. 2, pp.120–133, 2010.

[4] J. S. Han, C.S. Choi, and W.K Park. Smart home energy management system including renewable energy based on Zigbee and PLC. *IEEE Trans. Consumer Electron.*, vol. 60, no. 2, pp.198–202, 2014.
[5] Y. S. Son and K. D. Moon. Home energy management system based on power line communication. *IEEE Trans. Consumer Electron.*, vol. 56, no. 3, pp. 1380–1386, 2010.
[6] C. Chen, W. Jianhui, and H. Yeonsook. MPC-based appliance scheduling for residential building energy management controller. I*EEE Trans. Smart Grid*, vol. 4, no. 3, pp. 1401–1410, 2013.
[7] J. S. Byun, I.S. Hong, B. K. Kang, and S. H. Park. A smart energy distribution and management system for renewable energy distribution and context-aware services based on user patterns and load forecasting. *IEEE Trans. Consumer Electron.*, vol. 57, no. 2, pp. 436–444, 2011.
[8] P. Du and N. Lu. Appliance commitment for household load scheduling. *IEEE Trans. Smart Grid*, vol. 2, no. 2, pp. 411–419, 2011.
[9] A. Mohsenian-Rad, V. Wong, J. Jatskevich, R. Schober, and A. Leon-Garcia. Autonomous demand-side management based on game-theoretic energy consumption scheduling for the future smart grid. *IEEE Trans. Smart Grid*, vol. 1, no. 3, pp. 320–331, 2010.
[10] J. Contreras, R. Espinola, F. Nogales, and A. Conejo. Arima models to predict next-day electricity prices. *IEEE Trans. Power System.*, vol. 18, no. 3, pp. 1014–1020, 2003.
[11] D. M. Han and J. H. Lim. Smart home energy management system using IEEE 802.15.4 and Zigbee. *IEEE Trans. Consumer Electron.*, vol. 56, no. 3, pp. 1403–1410, 2010.
[12] P. Areekul, T. Senjyu, H. Toyama, and A. Yona. A Hybrid ARIMA and Neural Network Model for Short-term Forecasting in Deregulated Market. *IEEE Trans. Power System*, vol. 25, no. 1, pp. 524-530, 2010.
[13] Y. Chen, P. B. Luh, C. Guan, Y. Zhao, L. D. Michel, M. A. Coolbeth, P. B. Friedland, and S. J. Rourke. Short-Term Load Forecasting: Similar Day-Based Wave-let Neural Networks. *IEEE Trans. Power System*, vol. 25, no. 1, pp. 322–330, 2010.
[14] B. Li and A. G. Alleyne. Optimal On-Off Control of an Air Conditioning and Refrigeration System. *in Proc. Amer. Control Conf.*, pp. 5892–5897, 2010.
[15] D. Bargiotas and J. Birdwell. Residential air conditioner dynamic model for direct load control. *IEEE Trans. Power Del.*, pp. 2119–2126, 1988.
[16] Z. Yu, L. Jia, M. C. Murphy-Hoye, A. Pratt, and L. Tong. Modeling and Stochastic Control for Home Energy Management. *IEEE Trans. Smart Grid,* vol. 4, no. 4, pp. 2244-2255, 2013.
[17] M. A. A. Pedrasa, T. D. Spooner, and I. F. MacGill. Coordinated scheduling of residential distributed energy resources to optimize smart home energy services. *IEEE Trans. Smart Grid*, vol. 1, no. 2, pp. 134–143, 2010.
[18] C. K. Ahn. Robustness bound for receding horizon finite memory control: Lyapunov-Krasovskii approach. *International Journal of Control*, vol. 85, no. 7, pp. 942–949, 2012.
[19] C. K. Ahn, S. Han, and W. H. Kwon. H_∞ FIR filters for linear continuous time state-space systems. *IEEE Signal Process. Lett.*, vol. 13, no. 9, pp. 557–560, 2006.
[20] C. K. Ahn, S. Han, and W. H. Kwon. H_∞ finite memory controls for linear discrete-time state-space models. *IEEE Trans. Circuits and Systems II*, vol. 54, no. 2, pp. 97–101, 2007.
[21] Y. S. Shmaliy. Unbiased FIR filtering of discrete-time polynomial states pace models. *IEEE Trans. Signal Processing*, vol. 57, no. 4, pp. 1241–1249, 2009.
[22] J. M. Pak, C. K. Ahn, C. J. Lee, P. Shi, M. T. Lim, and M. K. Song. Fuzzy horizon group shift FIR filtering for nonlinear systems with Takagi Sugeno model. *Neurocomputing*, 174:1013–1020, 2016.
[23] J. M. Pak, C. K. Ahn, Y. S. Shmaliy, P. Shi, and M. T. Lim. Switching extensible FIR filter bank for adaptive horizon state estimation with application. *IEEE Trans. Control Systems Technology*, vol. 11, no. 5, pp. 1089–1098, 2015.
[24] J. M. Pak, C. K. Ahn, Y. S. Shmaliy, and M. T. Lim. Improving Reliability of Particle Filter-based Localization in Wireless Sensor Networks via Hybrid Particle/FIR Filtering. *IEEE Trans. Industrial Informatics*. vol. 11, no. 5, pp. 1089-1098, 2015..
[25] M. A. Piette, J. Granderson, M. Wetter, and S. Kiliccote. Intelligent building energy information and control systems for low-energy operations and optimal demand response. *IEEE Des. Test Comput.*, vol. 29, no. 4, pp. 8–16, 2012.
[26] K. M. Tsui and S. C. Chan. Demand response optimization for smart home scheduling under real-time pricing. *IEEE Trans. Smart Grid*, vol. 3, no. 4, pp. 1812–1821, 2012.
[27] S. Gokay, M. C. Beutel, H. Ketabdar, and K. H. Krempels. Connecting smart grid protocol standards: A mapping model between commonly used demand-response protocols OpenADR and MIRABEL. *in Proc. 4th International Conference on Smart Cities and Green ICT Systems.* 2015.
[28] S. Y. Son, S Koh, D. M. Son, D. Y. Hwang, and Y. H. Kim. A system model expansion for smart appliance demand response based on SEP 2.0. *in proc. IEEE International Conference on Consumer Electronics*, pp. 534-535, 2015
[29] M. Tariq, Z. Zhou, J. Wu, M. Macuha, and T. Sato. Smart grid standards for home and building automation. in Proc. *IEEE International Conference*

on Power System Technology, 2012.
[30] G. Ghatikar and R. Bienert. Smart grid standards and systems interoperability: a precedent with OpenADR. *in Proc. Grid-Interop Forum,* 2011.
[31] S. H. You, J. M. Pak, C. K. Ahn, P. Shi, and M. T. Lim. Unbiased Finite-Memory Digital Phase-Locked Loop. *IEEE Trans. Circuit and System,* vol. 63, no. 8, pp. 798-802, 2016.
[32] S. Zhao, Y. S. Shmaliy, and F. Liu. Fast Kalman-Like Optimal Unbiased FIR Filtering with Application. *IEEE Trans. Signal Processing,* vol. 64, no. 9, pp. 2284-2297, 2016.